Single-step superresolution by interferometric imaging

Vicente Mico

AIDO, Instituto Tecnológico de Óptica, Color e Imagen. C/. Nicolás Copérnico, 7-13
Parc Tecnològic - 46980 Paterna (Valencia) Spain

Zeev Zalevsky

School of Engineering, Bar Ilan University, Rama Gan, 52900 Israel

Pascuala Garcia-Martinez and Javier Garcia

Departamento de Optica. Universitat de Valencia. C/Dr.Moliner,50. 46100 Burjassot, Spain
javier.garcia.monreal@uv.es

Abstract: The use of vertical-cavity surface-emitting laser (VCSEL) arrays for implementation of incoherent source superresolution is presented. The method uses an interferometer setup to obtain superresolution in a single step. The novelty of the method relies on the use of a VCSEL array as the light source, which provides a set of coherent sources which are mutually incoherent. The technique accomplishes the transmission of several spatial frequency bands of the object's spectrum in parallel by use of spatial multiplexing that occurs because of the tilted illumination of the source array. The recording process is done by interference of each frequency band with a complementary set of reference plane waves. After the reconstruction process, the resolution of any optical system can approach the natural $\lambda/2$ limit. The benefit of our system is improved modulation speed and hence more rapid image synthesis. Moreover, any desired synthetic coherent transfer function can be realized at ultrafast rates if we simply change the electrical drive of the VCSEL array.

OCIS codes: (100.6640) Superresolution; (100.0100) Image processing; (110.0110) Imaging systems; (100.2000) Digital image processing; (090.0090) Holography

References and links

1. G. Toraldo di Francia, "Resolving power and information," J. Opt. Soc. Am. **45**, 497–501 (1955).
2. C. S. Chung and H. H. Hopkins, "Influence of non-uniform amplitude on PSF," J. Mod. Opt. **35**, 1485–1511 (1988).
3. J. Campos and M. J. Yzuel, "Axial and extra-axial responses in aberrated optical systems with apodizers. Optimization of the Strehl ratio," J. Mod. Opt. **36**, 733–749 (1989).
4. R. W. Gerchberg, "Super-resolution through error energy reduction," Opt. Acta **21**, 709–720 (1974).
5. W. Lukosz, "Optical sytems with resolving powers exceeding the classical limits. II," J. Opt. Soc. Am **57**, 932–941 (1967).
6. M. A. Grimm and A. W. Lohmann, "Superresolution image for one-dimensional objects," J. Opt. Soc. Am. **56**, 1151–1156 (1966).
7. A. W. Lohmann and D. P. Paris, "Superresolution for nonbirefringent objects," Appl. Opt. **3**, 1037–1043 (1964).
8. A. Shemer, D. Mendlovic, Z. Zalevsky, J. Garcia, and P. Garcia-Martinez, "Superresolving optical system with time multiplexing and computer decoding," Appl. Opt. **38**, 7245–7251 (1999).
9. E. Sabo, Z. Zalevsky, D. Mendlovic, N. Konforti, and I. Kiryuschev, "Superresolution optical system using three fixed generalized gratings: experimental results," J. Opt. Soc. Am. A. **18**, 514–520 (2001).
10. J. Salomon, Z. Zalevsky, and D. Mendlovic, "Superresolution by use of code division multiplexing," Appl. Opt. **42**, 1451–1462 (2003).

#4376 - $15.00 US Received 13 May 2004; revised 25 May 2004; accepted 25 May 2004

11. F. Le Clerc, M. Gross, and L. Collot, "Synthetic-aperture experiment in the visible with on-axis digital heterodyne holography," Opt. Lett. **26**, 1550–1552 (2001).
12. X. Chen and S. R. J Brueck, "Imaging interferometric lithography: approaching the resolution limits of optics," Opt. Lett. **24**, 124–126 (1999).
13. C. J. Schwarz, Y. Kuznetsova, and S. R. J. Brueck, "Imaging interferometric microscopy," Opt. Lett. **28**, 1424–1426 (2003).
14. E. N. Leith, D. Angell, and C.-P. Kuei, "Superresolution by incoherent-to-coherent conversion," J. Opt. Soc. Am. A **4**, 1050–1054 (1987).
15. P. C. Sun and E. N. Leith, "Superresolution by spatial-temporal encoding methods," Appl. Opt. **31**, 4857–4862 (1992).
16. A. Cunha and E. N. Leith, "Generalized one-way phase-conjugation systems," J. Opt. Soc. Am. B **6**,1803–1812 (1989).
17. P. Naulleau and E. Leith, "Imaging through optical fibers by spatial coherence encoding methods," J. Opt. Soc. Am. A **13**, 2096–2101 (1996).

1. Introduction

The ability to improve the resolving power of optical systems beyond the limits imposed by diffraction has long attracted considerable interest [1-9]. As a general rule, the numerical aperture (NA) determines the diffraction cutoff frequency of the systems, up to a maximum resolution of $\lambda/2$. Nevertheless, the use of optical systems with large NA (close to 1 in air) is costly and is not always possible. For this reason, superresolution systems have been proposed that produce a synthetic enlargement of an aperture without changing the aperture's physical dimensions. Some of the methods are based on the design of superresolving pupils to modify the axial or transverse response of optical systems [2,3]. Other methods are based on extrapolation of the information contained in the bandpass of the system and estimation of that information (as an example, see Ref. 4). Unless *a priori* information is added, the gain in resolution is modest.

A second family of methods to improve resolution relies on exploitation of an unused degree of freedom of the image to multiplex the spatial resolution of the image [1,5,6]. On this basis, one of the most appealing approaches for achieving resolving power, which exceeds the classical Rayleigh resolution limit given by the NA of the system, is related to temporally restricted objects and is based on two moving gratings [5,6]. The key idea is to introduce optical components, such as gratings or prisms [7], that will divert the higher spatial frequency components into the aperture of an optical imaging system. In particular, the first grating is responsible for encoding the input image, and the second performs the decoding operation. However, one of the main problems is synchronization between the gratings, which can be solved by replacement of the second moving grating with a virtual grating realized by digital processing with a computer [8]. Other superresolution methods can be found to avoid movement of the gratings by use of fixed gratings [9] or to applied code division multiplexing to superpose the high bands of information that are limited by the aperture of the imaging lenses [10]. Instead of deflecting the high frequencies into the system, it is possible to enlarge the synthetic aperture (SA) of the system by moving the aperture along one direction perpendicular to the system axis [11], although at the cost of a high-precision mechanical movement, which is also time-consuming .

Chen and Brueck [12] increased the spatial frequency coverage of conventional optical lithography by using an interferometric approach and Schwarz *et al*. [13] applied a similar concept to imaging interferometric microscopy. Off-axis illumination is used to downshift the high-frequency components generated with the object to low frequency where they can be collected by the lens, and interferometric optics shifts these components back to their original spatial frequencies at the image plane. Three individual exposures are coherent and the summation is made incoherently by means of a computer [13] or by use of different wavelengths for each exposure [12]. Thus a number of sequential exposures is needed to cover a sufficient region of frequency space to achieve a faithful image. The authors used only three exposures sequentially: one offset exposure in the *x* direction, one in the *y* direction, and one conventional exposure to provide the low-frequency information. Only one

#4376 - $15.00 US Received 13 May 2004; revised 25 May 2004; accepted 25 May 2004

side offset was used, since the object is assumed to be real. Although we used a simple standard binary mask, the complexity of the system is in correct alignment for the addition of three exposures. Moreover, different noise terms are recorded in the output plane superimposed onto the superresolved object.

In all the approaches the different spatial frequency components pass in a time sequence through an optical system after which the recorded intensities are added, resulting in an incoherent addition. The same effect from incoherent addition can be obtained by use of mutually incoherent light sources, one for each frequency slot. In this way all the spatial frequency slots are recorded in a single step.

Bearing this concept in mind, our proposal here is to use an array of vertical-cavity surface-emitting lasers (VCSELs) to illuminate an optical system. One can easily perform the selection of the central frequency of each band by changing the angle of the plane waves that illuminate the object. However, as reported in Refs. 12 and 13, it becomes necessary to change the angle of the reference waves that correspond to each change in angle of the object to carry out the superposition correctly. The proposed technique accomplishes the transmission of all the spatial frequencies transmitted at the same instant by use of spatial multiplexing of all the incoherent illumination sources. The recording process is done by interfering those spatial frequencies with multiple complementary reference planes at the same time. Moreover, the complexity of the system is not adversely affected by the additional frequency slots. Although the use of an incoherent source to increase the resolution of the imaging system was reported earlier by Leith *et al.* [14,15] and later was extended to include transmission of information through optical fiber [16,17], the combination of such a coding approach together with a VCSEL line array provided a variety of advantages. The VCSEL line array has two important features: First, the coherence length is close to the optical wavelength, i.e., the temporal variation of the relative phase is at the speed of light. In common systems one uses a diffuser to break the coherence of an optical source. Since its rotation speed is much slower than the speed of light, the coherence length is much larger than the optical wavelength. In our case a short coherence length is generated with high energetic efficiency and high optical intensity (each VCSEL in the array can go as high as 10 mW). Second, the VCSELs can be temporally modulated at modulation rates up to several gigahertz. Since the synthetic aperture generated by the suggested approach is actually a convolution of the VCSEL line array and the coherent transfer function (CTF) of the system, by temporally varying the relative amplitudes of each source in the line array, one can realize any synthetic transfer function at will. Thus, an ultrafast (at a gigahertz rate) tunable filter can be generated. As mentioned above, since the coherence length is short and despite the gigahertz rate amplitude modulation, the sources still remain incoherent and the operating principle is not compromised. The ability to realize an ultrafast tunable filter also makes the suggested approach applicable for optical recognition of patterns with simultaneous invariant properties. With respect to the method in Ref. 13, the main advantage of our method is the ease of using an arbitrarily large number of frequency channels, with no adverse effect on the complexity of the system. Note that, since the VCSEL can contain a large number of elements (hundreds), the suggested system transmits a broader part of the spatial frequency spectrum and thus the resolution limit is enhanced. Here we demonstrate the concept for as many as five simultaneous sources in comparison with the three illumination angles reported for the system in Ref . 13.

2. Theoretical analysis of the optical setup

The concept of the proposed method can be easily understood from the optical setup shown in Fig. 1. The system is analogous to a Mach–Zehnder interferometer and is used to demonstrate the performance of the method experimentally.

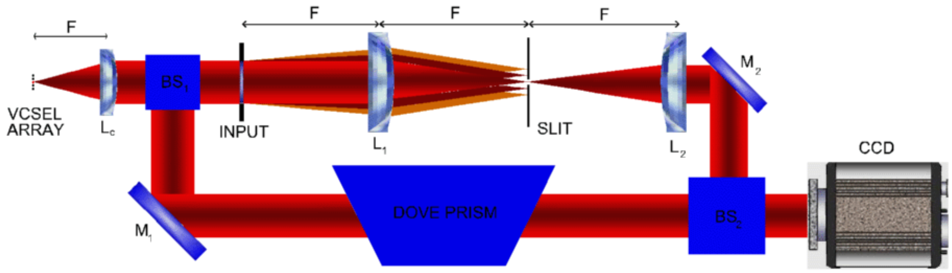

Fig. 1. Experimental setup (260 Kbytes). The actual experiment uses five VCSELs lit simultaneously, although the movie presents the lighting of the VCSELs in a time sequence for clarity.

Light from a VCSEL array passes through a collimation lens (L_c) and produces a set of parallel beams with different orientations that illuminate the object. The object is imaged through two identical lenses (L_1 and L_2) in a 4*f* configuration onto a CCD camera. Two beam splitters (BS_1 and BS_2) bend the optical path and allow the separation and later recombination of a reference beam for each VCSEL. The reference arm of the system must have the same angular magnification as the imaging arm. With an image magnification of -1, one can use a dove prism to invert the angles in the reference so that they equal the angles in both paths. A bias in the carrier frequency of the interference pattern can be achieved by slightly tilting mirror M_1 or M_2.

To demonstrate the method, we reduce the system aperture by adding a slit in the Fourier plane of lens L_1. We define the input as $f(x)$ and $\tilde{f}(\nu)$ is the Fourier transform, where x and ν are the spatial and spatial-frequency coordinates, respectively. A rectangular pupil of size $\Delta\nu$ acts as the CTF at the Fourier plane, so the amplitude distribution in the CCD from the upper branch of our optical system is a low-pass version of input

$$U_{CCD}^{on-axis}(x) = f(x) \otimes sinc(x\Delta\nu). \tag{1}$$

In Eq. (1) we consider only the on-axis illumination, so only the central VCSEL is on. Note that ⊗ denotes a convolution operation. The Fourier transform of the input object can be split into slots as

$$\tilde{f}(\nu) = \sum_{m=-\infty}^{+\infty} \tilde{f}(\nu) rect\left(\frac{\nu - m\Delta\nu}{\Delta\nu}\right). \tag{2}$$

We assume that the VCSELs are separated to produce spacing $\Delta\nu$ in the Fourier domain (all the computations are done in normalized units of λF, where λ is the wavelength of the illumination and F is the focal length of various lenses). Then VCSEL number m illuminates the input with an inclined plane wave $exp[j2\pi m\Delta\nu x]$ and so the complex amplitude at the Fourier plane that corresponds to the *m*th VCSEL is

$$\tilde{U}_m(\nu) = \tilde{f}(\nu - m\Delta\nu) Rect\left(\frac{\nu}{\Delta\nu}\right). \tag{3}$$

The Fourier transform of Eq. (3) gives the contribution at the image plane:

$$U_m(x) = \left[f(-x) e^{-j2\pi m\Delta\nu x}\right] \otimes sinc(x\Delta\nu). \tag{4}$$

Each m VCSEL source creates a different plane wave from the reference arm of the setup. The advantages of this system in comparison with previous systems [11,12] is that there is no

#4376 - $15.00 US
Received 13 May 2004; revised 25 May 2004; accepted 25 May 2004

need to adjust the inclination of the plane wave and thus the carrier frequencies. Moreover, in our system at the CCD camera we found the incoherent addition of each *m* VCSEL in a single step. No need to add the *m* distributions *a posteriori*.

The intensity distribution at the CCD from this input and from the reference illumination for one source is

$$
\begin{aligned}
I_m(x) &= \left|\left[f(-x)e^{-j2\pi m\Delta\nu x}\right]\otimes \sin c\left(x\Delta\nu\right)+e^{-j2\pi(m\Delta\nu+Q)x}\right|^2 = \\
&= 1+\left|\left[f(-x)e^{-j2\pi m\Delta\nu x}\right]\otimes \sin c\left(x\Delta\nu\right)\right|^2 \\
&\quad +\left[f(-x)e^{-j2\pi m\Delta\nu x}\right]\otimes \sin c\left(x\Delta\nu\right)\times e^{j2\pi(m\Delta\nu+Q)x} \\
&\quad +\left[f^*(-x)e^{j2\pi m\Delta\nu x}\right]\otimes \sin c\left(x\Delta\nu\right)\times e^{-j2\pi(m\Delta\nu+Q)x}.
\end{aligned}
\tag{5}
$$

Note that the reference VCSEL *m* is $\exp[-j2\pi(m\Delta\nu+Q)\,x]$, where *Q* is the bias carrier frequency. This *Q* value must be larger than half of the size of the pupil plus the size of one slot, where *N* is the number of slots. So, $Q\geq\Delta\nu\times(N/2+1)$.

We refer to the four terms in Eq. (5) as $T_1(x)$, $T_2(x)$, $T_3(x)$, and $T_4(x)$. After the intensity $I_m(x)$ is stored, we perform digitally an inverse Fourier transformation. The Fourier transform of the first term [$\tilde{T}_1(\nu)$] is a delta function centered at the origin. The second term, also centered at the origin, is the centered autocorrelation of the bandpass slot (with width $2\Delta\nu$):

$$
\tilde{T}_2(\nu)=\left[\tilde{f}(\nu-m\Delta\nu)rect\left(\frac{\nu}{\Delta\nu}\right)\right]*\left[\tilde{f}(\nu-m\Delta\nu)rect\left(\frac{\nu}{\Delta\nu}\right)\right],
\tag{6}
$$

where $*$ denotes correlation. $\tilde{T}_3(\nu)$ is the *m*th slot at its left position plus an offset -*Q*:

$$
\begin{aligned}
\tilde{T}_3(\nu) &= \left[\tilde{f}(\nu-m\Delta\nu)\times rect\left(\frac{\nu}{\Delta\nu}\right)\right]\otimes\delta\left(\nu+m\Delta\nu+Q\right) \\
&= \left[\tilde{f}(\nu)\times rect\left(\frac{\nu+m\Delta\nu}{\Delta\nu}\right)\right]\otimes\delta\left(\nu+Q\right).
\end{aligned}
\tag{7}
$$

Analogously, $\tilde{T}_4(\nu)$ is the same as Eq. (7) but at the right-hand side position:

$$
\tilde{T}_4(\nu)=\left[\tilde{f}^*(\nu)\times rect\left(\frac{\nu-m\Delta\nu}{\Delta\nu}\right)\right]\otimes\delta\left(\nu-Q\right)
\tag{8}
$$

We now consider the output when the full VCSEL array is activated. Owing to the mutual incoherence of the holograms, the output is the addition of all the terms in Eq. (5) for all the VCSELs. The contribution of the third term for all VCSELS is

$$
\tilde{T}_{3\Sigma}(\nu)=\sum_{m=-\infty}^{\infty}\left[\tilde{f}(\nu)\times rect\left(\frac{\nu+m\Delta\nu}{\Delta\nu}\right)\right]\otimes\delta\left(\nu+Q\right)=\tilde{f}(\nu)\otimes\delta\left(\nu+Q\right).
\tag{9}
$$

The last term can be isolated and centered digitally (thus removing the delta function). A new Fourier transform recovers $f(-x)$, so the input object can be completely reconstructed. Also, note that the fourth term [Eq. (8)] appropriately centered and Fourier transformed will give the complex conjugate of the inverted image. Note that Eq. (9) can be rewritten as

#4376 - $15.00 US Received 13 May 2004; revised 25 May 2004; accepted 25 May 2004

$$\tilde{T}_{3\Sigma}(\nu) = \left\{ \tilde{f}(\nu) \left[rect\left(\frac{\nu}{\Delta \nu} \right) \otimes \sum_{m=-\infty}^{\infty} \left[\delta(\nu + m\Delta\nu) \right] \right] \right\} \otimes \delta(\nu + Q) . \tag{10}$$

The last delta function is just a shift of the signal spectrum, whereas the term in square brackets is the SA of the system:

$$SA(\nu) = rect\left(\frac{\nu}{\Delta \nu} \right) \otimes \sum_{m=-\infty}^{\infty} \left[\delta(\nu + m\Delta\nu) \right] . \tag{11}$$

Thus the SA generated by the suggested approach is actually the convolution of the VCSEL line array and the CTF of the system. Within the limit of VCSEL spacing approaching zero, the VCSEL array behaves like an incoherent extended source [14]. In a general case, the SA is the convolution of the CTF and the function that describes the light density of the source. The use of a VCSEL array provides the flexibility of tailoring the SA by programming the intensity of each VCSEL in the array.

Note that no assumption about properties of $f(x)$ is made, so for any complex input distribution we would always reconstruct that input. This advantage is important for application in microscopy, three-dimensional imaging, or invariant pattern recognition.

3. Experimental results

The proposed superresolution method has been experimentally tested in the optical system shown in Fig. 1. For the experiments we used as many as five VCSELs separated by a 500-μm pitch. This array of sources is monochromatic with $\lambda = 850nm$. Without the slit in the Fourier plane that limits the aperture, the system has unity magnification and a NA of 0.12. Owing to the unity magnification, the resolution of the unobstructed system is higher than that of the CCD detector. Thus, to demonstrate the method, the resolution capability of the system is reduced by means of the Fourier plane slit. We used two test objects: the first was a 25-μm-wide slit and the second was a resolution test. As a reference, high-resolution coherent images of the test objects, without limitation in the Fourier plane, are shown in Fig. 2.

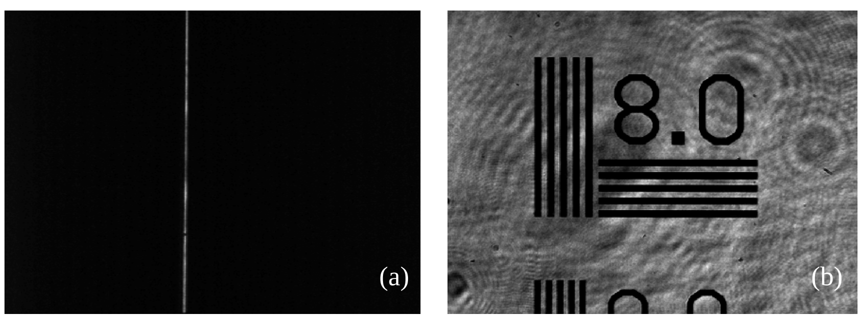

Fig. 2. Test objects of (a) the slit and (b) the resolution test

The hologram of the slit object [as described in Eq. (5)] by use of five sources is shown in Fig. 3(a), whereas the Fourier transform of the slit hologram is shown in Fig. 3(b). One can observe the four additional terms: $\tilde{T}_1(\nu)$, $\tilde{T}_2(\nu)$, $\tilde{T}_3(\nu)$, and $\tilde{T}_4(\nu)$. The region of interest is marked in Fig. 3(b). For the reconstruction the values outside the region of interest are not considered.

#4376 - $15.00 US Received 13 May 2004; revised 25 May 2004; accepted 25 May 2004

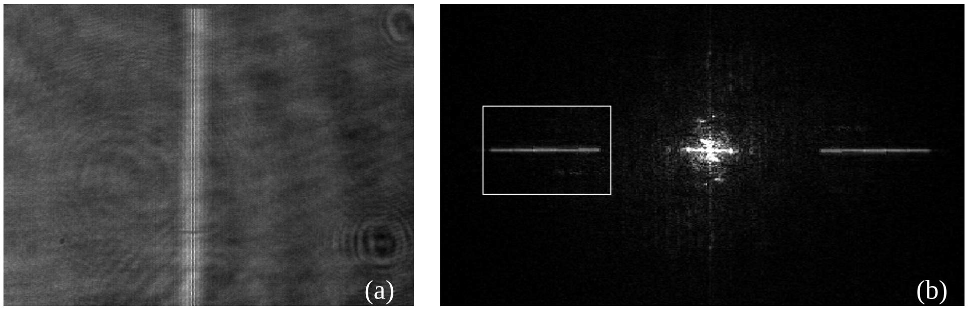

Fig. 3. (a) Image recorded in the CCD [Eq. (5)] and (b) inverse Fourier transform of (a) performed digitally.

A second Fourier transform of the region of interest yields the reconstruction of the object. In Fig. 4(a) we show the reconstructed input obtained with the superresolution approach, whereas Fig. 4(b) shows the image given by the imaging system with a limited aperture; see Eq. (4). As can easily be seen, an impressive superresolution effect was obtained.

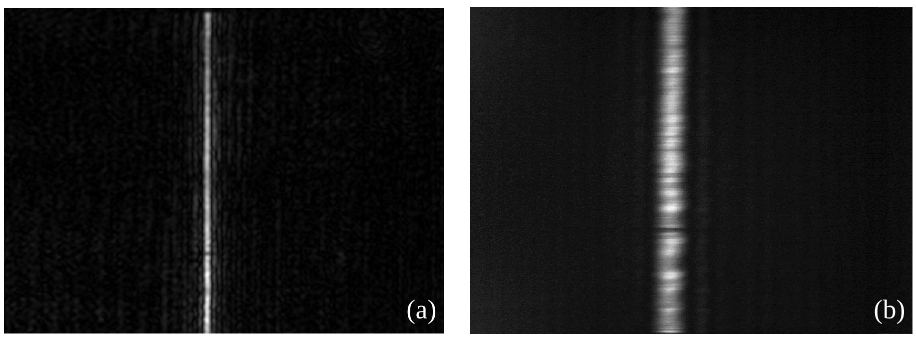

Fig. 4. (a) Superresolved image of the slit and (b) conventional image with a limited aperture.

In Fig. 5 we show the experimental results of the resolution test. The conventional test image with a limited aperture is shown in Fig. 5(a). Note that, because the array of sources is along an axis and the pupil has only one dimension, the superresolution approach affects only the horizontal direction. For the orthogonal axis, there is no need to superresolve the image because there is no limitation in the Fourier plane. However, the superresolution improvements are easily recognizable even for the number 8.0.

Moreover, as mentioned in Section 1, one of the main advantages of our method is the ease of using an arbitrarily large number of frequency channels, with no adverse effect on the complexity of the system. This can be achieved if different amounts of VCSELs are activated. In Fig. 5(b) we show the resolved image obtained with three VCSELs, and in Fig. 5(c) the same resolution test obtained with five VCSELs activated. Note the differences between Figs. 5(b) and 5(c), in particular the lower details of the test are resolved only by use of five VCSELs . As we increased the number of VCSELs, a large number of frequency channels were taken into account, so the resolution of the system increased. We can also provide a high-pass version of the test [Fig. 5(d)] simply by switching off the axial VCSEL (four off-axis VCSELs remain on).

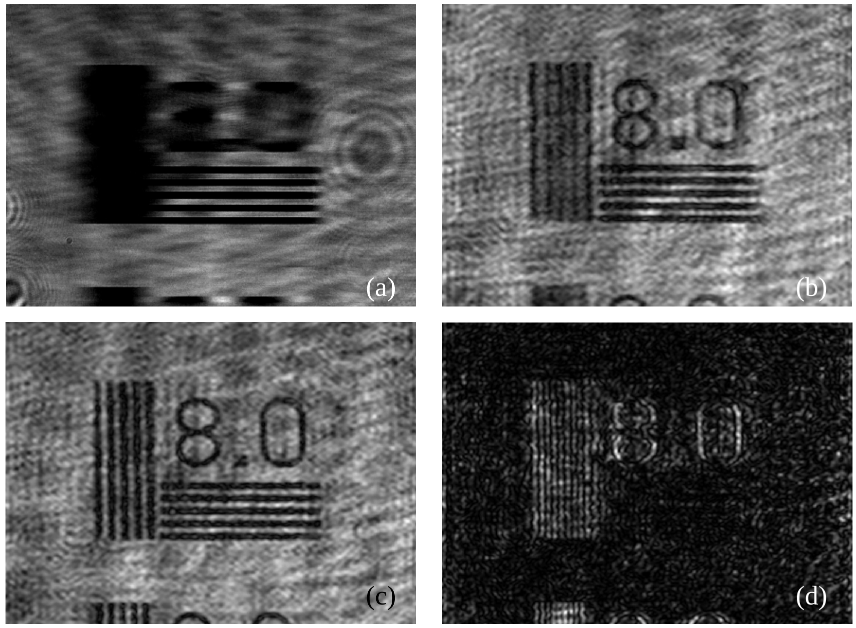

Fig. 5. (a) Conventional image with a limited aperture (only axial source). (b) Output with the superresolution approach with three sources. (c) Output with the superresolution approach with five sources. (d) High-pass version obtained as for (c) but with the central source turned off.

4. Conclusion and discussion

We have presented a superresolution approach based on an array of mutually incoherent sources. The idea is based on multiple superpositions of digital image holograms having different carrier frequencies in parallel. The spatial frequency bands are transmitted through a lens with different illumination sources, and this information is recorded by an interferometric process with reference waves generated by the point sources themselves. Finally we recorded a hologram and digitally processed it by use of two Fourier transforms. With respect to former superresolution methods based on an interferometric procedure with coherent sources, our method has the advantage of using a single-step exposure without changing the setup, eliminating the need for multiple exposures to vary the inclination of the reference waves. Moreover no assumption about the object is done, so the method can be used for more complicated objects, even phase objects. These advantages are also shared by superresolution methods based on incoherent sources. Nevertheless, the use of a VCSEL line array has major advantages, the main ones being an increase in illumination and the possibility of modulating the light sources. We used a one-dimensional VCSEL array, but the superresolution can be obtained in both directions by use of commercially available two-dimensional arrays. The use of VCSELs allows for the realization of tunable filters at gigahertz modulation rates and use of the approach for invariant pattern recognition and real-time image enhancements.

Acknowledgments

This research was supported by FEDER funds, the Spanish Ministerio de Ciencia y Tecnología, project BFM2001-3004, and the Agencia Valenciana de Ciencia y Tecnología (AVCT), project GRUPOS03/117.